ELSEVIER

S0032-3861(96)00513-7

*Polymer* Vol. 38 No. 2, pp. 297–307, 1997

0032-3861/97/$17.00 + 0.00

# AFM study of thermotropic structural transitions in poly(diethylsiloxane)

**S. N. Magonov* and V. Elings**
*Digital Instruments Inc., 520 E. Montecito St., Santa Barbara, CA 93103, USA*

**and V. S. Papkov**
*Institute of Organoelement Compounds, Russian Academy of Sciences, 28 Vavilov St., 117813 Moscow, Russia*
*(Received 15 February 1996; revised 23 March 1996)*

Structure and phase transitions of polydiethylsiloxane (PDES) were studied with AFM at temperatures in the 300–268 K range. The measurements were performed on a polymer layer deposited on a Si substrate by rubbing. It is shown that at room temperature the layer is a polymer mixture in amorphous and mesomorphic states. With the decrease of temperature to 273 K, all material converts into the mesomorphic state. The polymer structure in the mesomorphic state is formed of elongated patterns oriented perpendicular to the rubbing direction. They are assigned to edge-on standing and flat-lying lamellae. Disk-like substructures were found in some amorphous patches lying on the substrate. Solid–solid crystallization of PDES from the mesomorphic state was observed at 268 K. The transition is accompanied by changes of sample morphology and nanostructure. Lamellar arrays are transformed into ribbons whose shape reveals their monoclinic crystalline structure. The ribbons have a linear substructure with 50 nm wide stripes oriented along the rubbing direction. The molecular rearrangements during crystallization are discussed. Copyright © 1996 Elsevier Science Ltd.

**(Keywords: poly(diethylsiloxane); mesomorphic state; crystallization; AFM)**

## INTRODUCTION

Since the advent of atomic force microscopy (AFM) this method has often been applied to examine surface morphology, nanostructure and chain order of polymer samples[1]. These applications have demonstrated the unique potential of AFM for surface characterization of polymers and also has revealed definite limitations, mostly related to possible damage of soft polymer materials[2]. Therefore, consideration of tip-sample force interactions and optimization of the experimental conditions is required to obtain reliable information from AFM images[3]. Low-force imaging is required for a non-destructive examination of surface morphology and nanostructure. Measurements at different forces provide access to nanomechanical properties of polymers[4].

The necessity to avoid surface damage to soft samples led to the development of TappingMode™ (Digital Instruments, Santa Barbara, CA)[5]—the most popular mode among AFM modulation techniques[6]. In this mode, the decrease of amplitude of the oscillating probe due to tip-sample force interactions is employed for surface imaging. The short, intermittent tip-sample contact prevents inelastic surface deformation. TappingMode is indispensable for soft samples, which cannot be examined with the AFM mode contact. In addition, detection of phase shifts of the probe oscillation provides enhanced contrast for nanoscale features. Under certain circumstances the contrast of the images representing phase shifts (i.e. 'phase images') is related to surface stiffness[4]. The results presented below confirm the importance of phase imaging in AFM of polymers.

Poly(diethylsiloxane), PDES, is a polymer with a flexible inorganic backbone $[-Si(C_2H_5)_2-O-]_n$, which exists in different structural states[7]. According to the calorimetric and X-ray diffraction data[8], at temperatures below 280 K PDES is in a crystalline state, and above 320 K it is in an amorphous state. In the intermediate temperature range this polymer is in a mesomorphic state. N.m.r. and dynamic mechanical studies of different PDES samples[7b] revealed a high level of molecular mobility in the mesomorphic state with frequencies in the 1–100 Hz range. These relaxations were assigned to rotational reorientation of methyl groups and backbone motion. Structural characterization of PDES was also performed with optical and electron microscopy[9]. Electron microscopy of this polymer in the mesomorphic state revealed a variety of elongated structures, which were assigned to lamellar aggregates. The width of individual lamellae varied from 50–70 nm to 150–300 nm depending on the thermal history of the polymer sample. The molecular organization of PDES in the mesomorphic state is not well understood. It was first explained as a conformational disordered crystal, and later as a hexagonal columnar state[9].

This paper shows that the use of the TappingMode with phase imaging allows one to visualize morphology and nanostructure of PDES samples. PDES cannot be

* To whom correspondence should be addressed

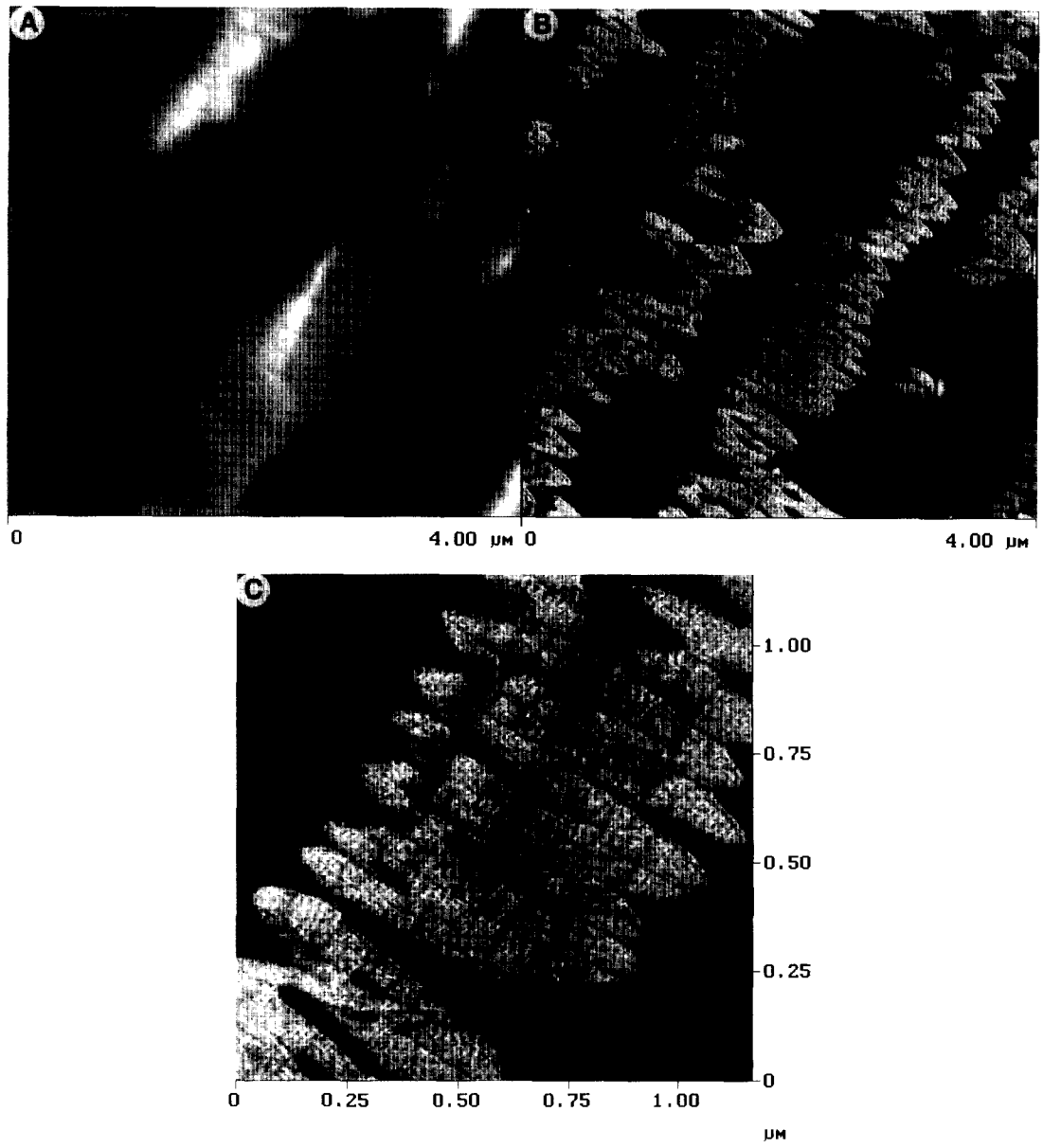


**Figure 1** (A)–(B) Simultaneously recorded AFM height and phase images of oriented PDES samples. (C) Phase image of the part of the sample shown in (A)–(B). The contrast covers height variations in the 0–100 nm scale in (A) and phase variations in the 0–50° range in (B), and in the 0–40° range in (C). Rubbing direction is from lower left to upper right

examined in AFM contact mode due to its softness. The measurements were conducted at temperatures in the 300–268 K range, and for the first time thermotropic structural transitions in a polymer sample were monitored with AFM.

## EXPERIMENTAL

For the present study a sample of PDES[8] with intrinsic viscosity $[\eta] = 0.58\,\mathrm{dl\,g^{-1}}$ (in toluene at 300 K) and molecular weight $M_w = 1.62 \times 10^5$ was used. At room temperature (RT), PDES is a soft, highly viscous material. For AFM imaging it was deposited on a piece of Si wafer by rubbing at RT. This procedure is often used to orient polymers, and leads to perfect molecular chain orientation of polytetrafluoroethylene as proven by AFM[11].

AFM measurements were conducted with a scanning probe microscope (Nanoscope® IIIa Multimode™, Digital Instruments, Santa Barbara, CA) by using TappingMode with phase imaging. An optical microscope combined with the Nanoscope was useful for positioning the probe on oriented PDES patches in surface regions with a low polymer coverage. As will be seen from the AFM images presented below, the thickness of such polymer layers is in the 50–150 nm range. Si probes with 125 $\mu$m long cantilevers (Nanoprobes®,

**Figure 2** (A)–(B) Low-force AFM height and phase images of an oriented PDES sample recorded at RT. (C)–(D) High-force AFM height and phase images of the same place as in the images in (A)–(B) recorded at RT. The cross-section profiles along the a–a lines are shown above the height images. The contrast covers height variations in the 0–200 nm range in (A) and phase variations in the 0–50° range in (B). Rubbing direction is from lower left to upper right. Markers in the cross-section profiles show a relative height of a spot indicated with an arrow in (A–D)

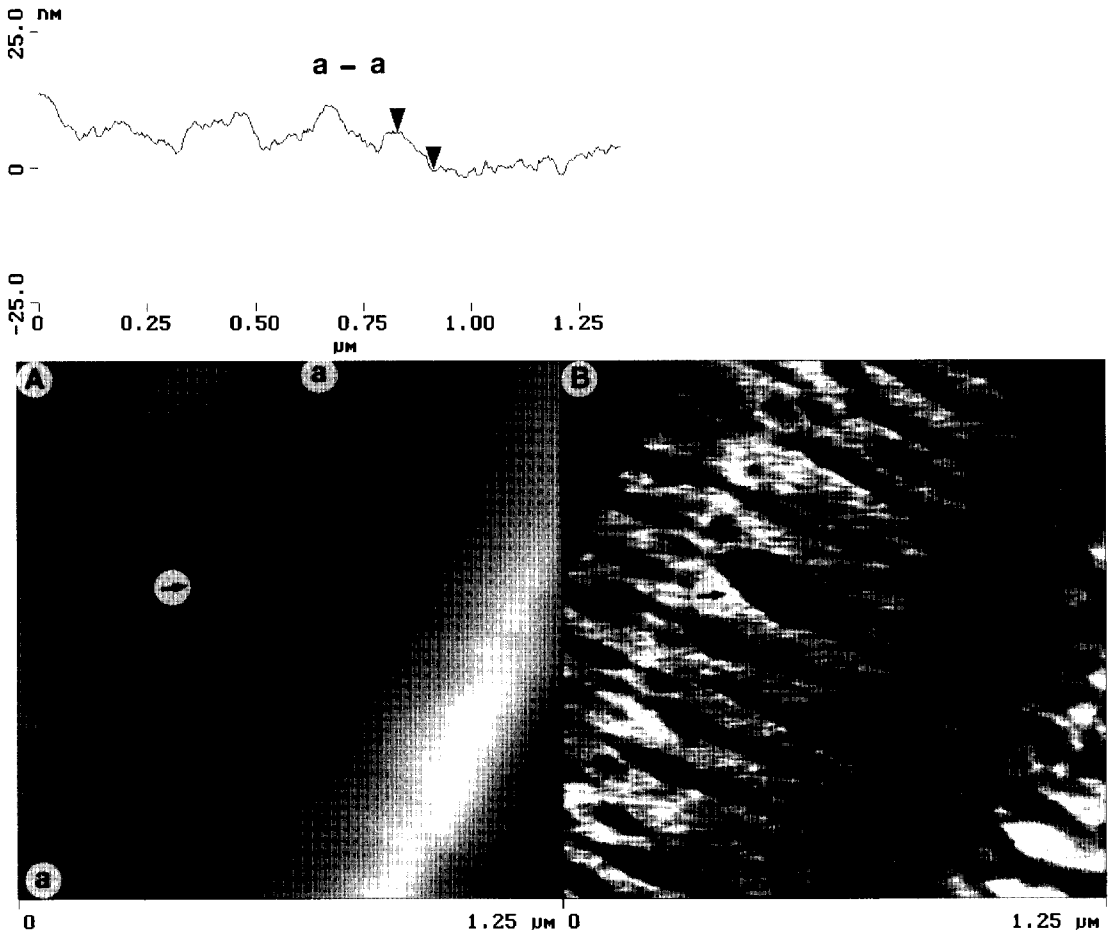
25.0 nm
a – a
0
-25.0
0
0.25
0.50
0.75
1.00
1.25
μm
A
a
B
c
a
0
1.25 μm 0
1.25 μm

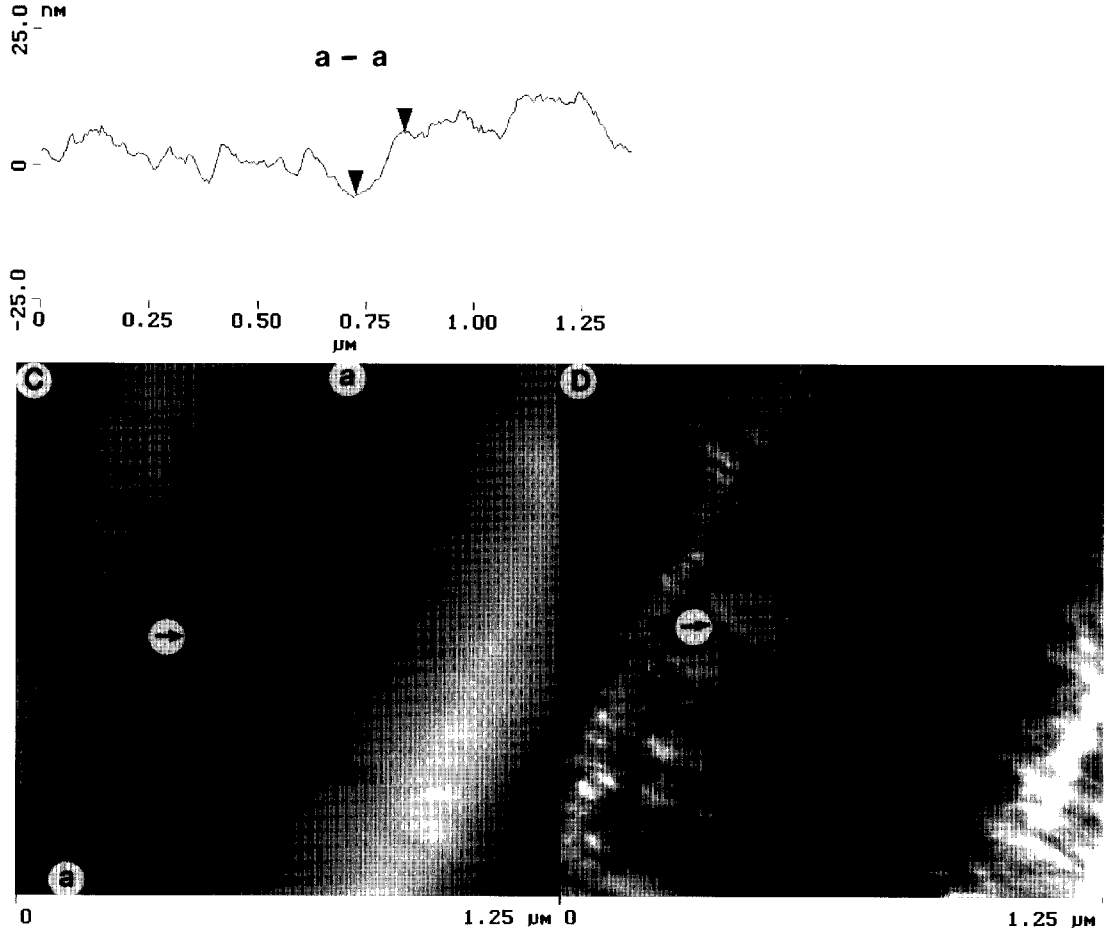
25.0 nm
a – a
0
-25.0
0
0.25
0.50
0.75
1.00
1.25
μm
C
a
D
c
c
a
0
1.25 μm 0
1.25 μm

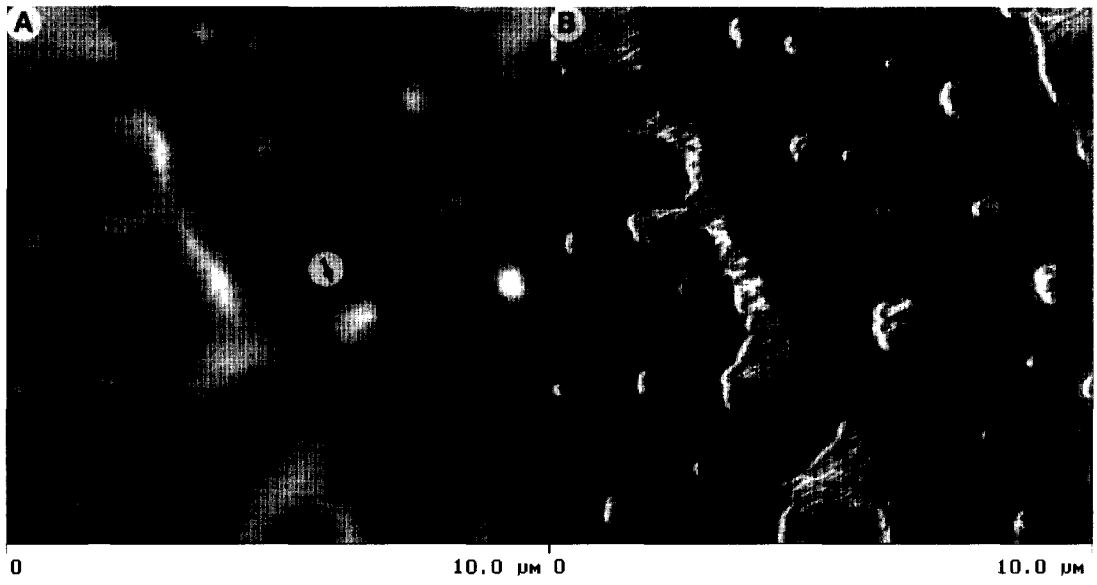


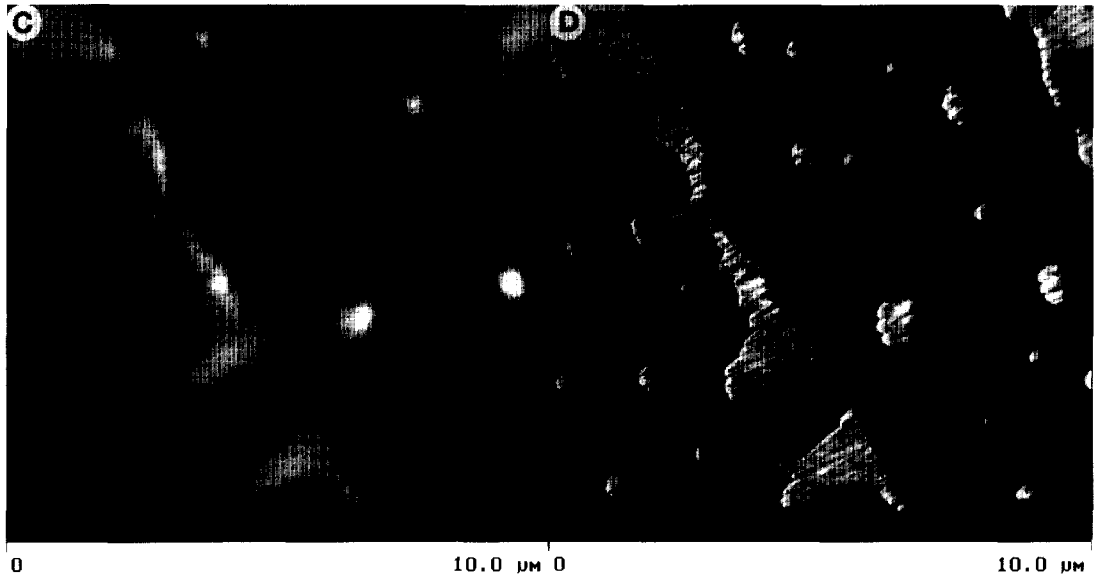


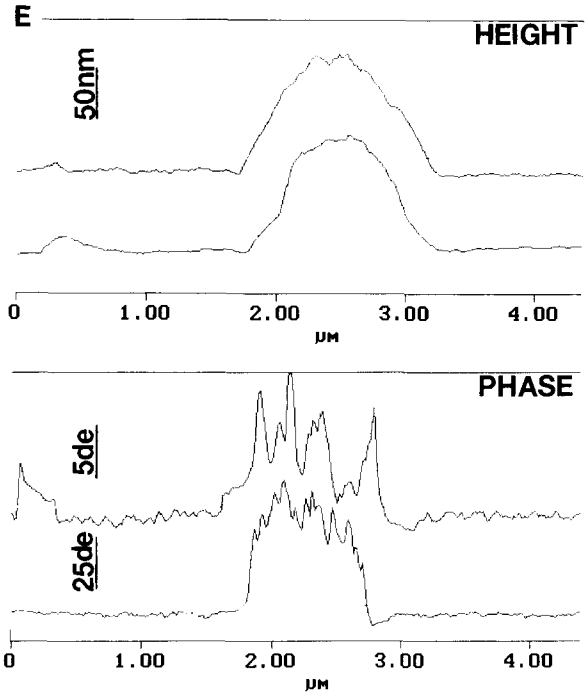


**Figure 3** (A)–(B) Low-force AFM height and phase images of PDES measured at 1.7 MHz. (C)–(D) High-force AFM height and phase images of the same place as in (A)–(B) measured at 1.7 MHz. (C) Cross-sectional height (upper part) and phase (lower part) profiles along a PDES patch indicated with an arrow in (A). For comparison the height and phase profiles obtained in low-force imaging are shown above those recorded in high-force imaging. The contrast covers height variations in the 0–270 nm range in (A) and (C), and phase variations in the 0–20° range in (B) and in the 0–60° range in (D). In all images the rubbing direction is from lower right to upper left

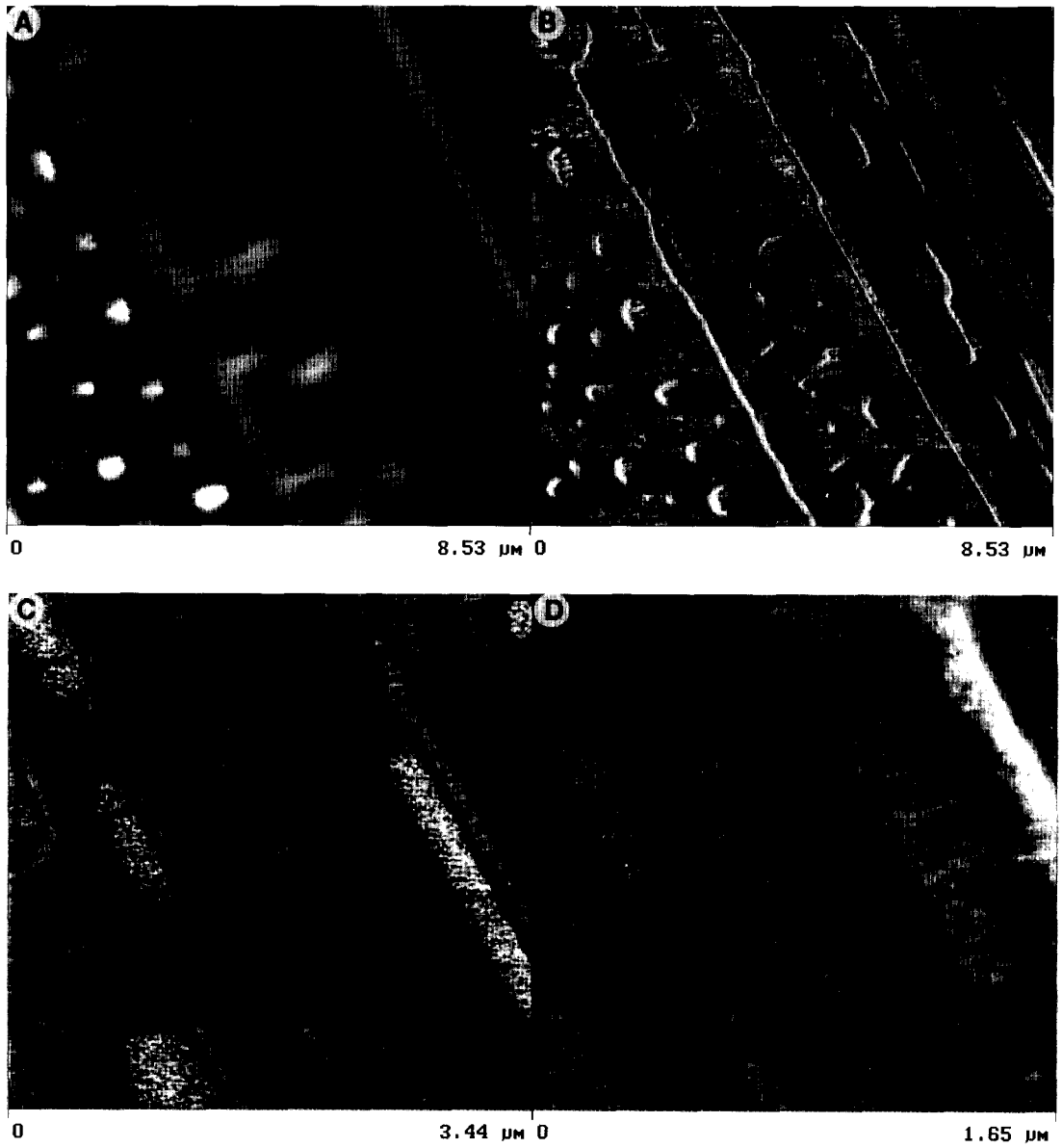


**Figure 4** (A)–(B) AFM height and phase image of PDES sample at room temperature. (C) Phase image of a part of the area in (A)–(B) showing nanostructure of PDES in the mesoscopic state at room temperature. (D) Phase image of a part of the area in (A)–(B) showing nanostructure of PDES in the mesoscopic state at 278 K. The contrast covers height variations in the 0–180 nm range in (A), phase variations in the 0–30° range in (B), and in the 0–40° range in (C), and in the 0–25° range in (D). In all images the rubbing direction is from lower right to upper left

Digital Instruments) were used in the experiments, and the imaging was conducted at their fundamental resonance frequency (250–300 kHz). In some cases, imaging at the second resonance frequency (1.5–1.8 MHz) was also performed[4].

We simultaneously recorded the height and phase images. The latter present the phase variations of the oscillating cantilever determined at its free resonance frequency. The height images reveal surface topography, whereas structural features on the nanometre scale are better resolved in the phase images. The phase contrast correlates with variations of surface stiffness when measurements are performed at different levels of the tip-sample force. For TappingMode imaging at different forces, the set-point amplitude, which is used for feedback control, was changed from 60–80% (low-force imaging) to 10–20% (high-force imaging) of the amplitude of the free-oscillating cantilever. Unless specifically stated, the images shown were obtained by low-force imaging at the fundamental frequency.

To perform measurements from RT to 283 K the microscope head was put into a thermoelectrically cooled box. Further cooling was done by purging with cold nitrogen. The temperature changed *ca.* 2°C $min^{-1}$ before it reached 268 K, at which temperature the PDES was crystallized. The imaging was performed continously during cooling.

## RESULTS AND DISCUSSION

In the presentation of the experimental results, we will first discuss phase imaging, then the morphology and nanostructure of PDES samples in the amorphous and mesomorphic states, and finally, the thermotropic transition from the mesomorphic to the crystalline state.

### *Phase imaging*

The advantage of phase imaging is clearly seen from the images in *Figures 1A–1B*, which were recorded on the surface of oriented PDES layer. The height image in

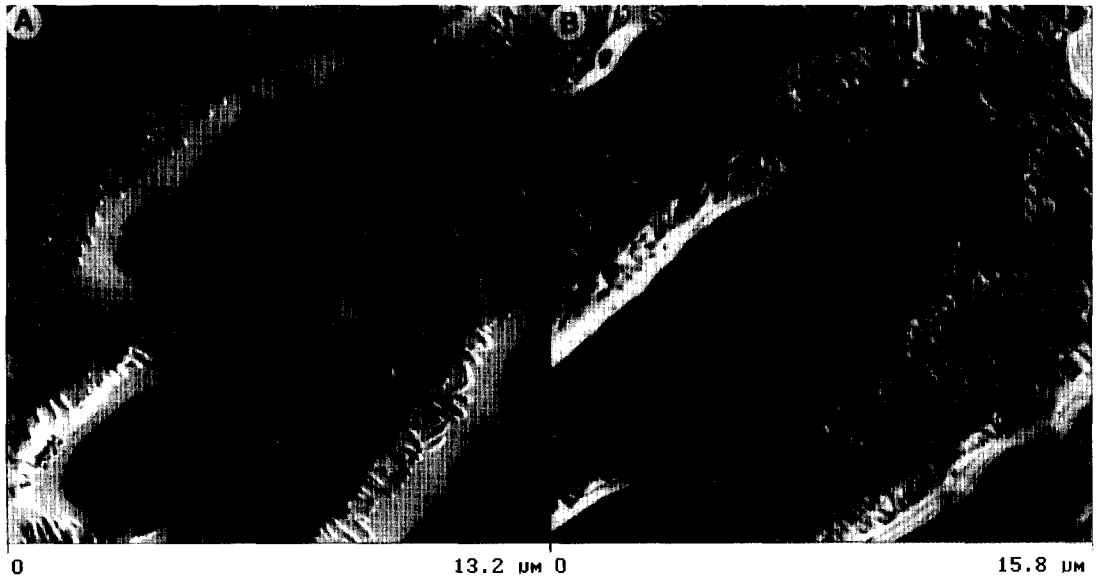


**Figure 5** (A)–(B) AFM phase images of a PDES sample at RT and 283 K, respectively. The contrast covers phase variations in the 0–75° range in (A) and in the 0–90° range in (B). Rubbing direction is from lower left to upper right

*Figure 1A* demonstrates the corrugated morphology of this layer with strands extending along the rubbing direction. The PDES strands are up to 70 nm in height. The phase image distinctively shows elongated nanostructures, which are only vaguely seen in the height image. The nanostructures are of 80–120 nm in width and up to 1 $\mu$m in length, and are oriented perpendicular to the rubbing direction. They have sharp edges, and many of them are connected to each other or even merge together, thus forming continuous aggregates. In the higher magnification phase image (*Figure 1c*) one sees that the nanostructures exhibit fine linear features with widths in the 10–20 nm range, which are aligned perpendicular to the rubbing direction.

As indicated above one can expect that at RT the sample is a mixture of polymer in the amorphous and mesomorphic states. The structures found in the mesomorphic state by optical and electron microscopy were assigned to lamellar aggregates[8a,9]. Therefore, nanostructures seen in the AFM images can be also assigned to polymer lamellae. As shown below, the shape and size of the lamellae found in the phase images of other PDES strands can be different, but they are always oriented perpendicular to the rubbing direction. In the isotropic films (thickness of *ca.* 300 $\mu$m), PDES lamellae did not exhibit a preferential orientation[9].

The fact that the lamellar structure of PDES in the mesomorphic state is better resolved in the phase images is most likely due to their stiffness being greater than that of the amorphous polymer. This is confirmed by the following considerations: in the recent AFM study of a multilayer polymer sample, which consists of alternating layers of polyethylene (PE) with different density, it was shown that the contrast of the phase image correlates with polymer stiffness. Low-force imaging of hard layers of high density PE exhibits brighter contrast in the phase image than soft layers of low density PE, and this contrast is reversed in the high-force image[4]. A similar trend is found in the imaging of PDES strands shown in *Figures 2A–D*. Linear nanostructures, 30–60 nm in width, which form a skeleton of this strand, are seen brighter than their surroundings in the low-force phase image, *Figure 2B*. The contrast is reversed in the high-force phase image, *Figure 2D*. This finding justifies assignment of the nanostructures to lamellae of PDES in the mesomorphic state, and their surroundings to amorphous polymer.

In contrast to the phase images where the force-dependent changes are pronounced, only minor effects can be seen in the height images. Specifically, the spot (indicated by arrows in *Figures 2A* and *2C*) which belongs to the amorphous PDES is slightly darker than neighbouring structures in the high-force height image. To better illustrate this effect, we present the cross-section height profiles along the a–a lines, which are shown above the height images. From these profiles it is clear that the tip-force caused a compression of the amorphous polymer. This effect became more evident in the measurements at the second resonance frequency of Si cantilevers, as seen from the low- and high-force images in *Figures 3A–D*. We conclude that imaging at the second resonance frequency induces greater tip-sample due to higher effective spring constant of the cantilever (relative to the fundamental resonance frequency). From *Figure 3* it is evident that with the force increase, the height and phase images are changing as emphasized in the cross-section profiles along the PDES patch (indicated with an arrow in *Figure 3A*), which are shown in *Figure 3E*. In the high-force image the height profile exhibits lower sides than those in the low-force height profile. This can be explained by a compression of the amorphous polymer surrounding the PDES lamellae, which is seen as a darker border around the polymer patches in the phase image (*Figure 3B*). The border as well as some patches of amorphous polymer, are almost invisible in the high-force phase image (*Figure 3D*). To summarize, the bright patterns seen in the high-force height and phase images represent lamellar arrays of PDES in the mesomorphic state*.

* The fact that the lamellar arrays exhibit bright contrast does not contradict the observation in *Figure 2D*, where the similar structures exhibit darker contrast than the amorphous polymer. In the case of a substantial compression of the thin amorphous layer, its stiffness is likely defined by the rigid underlying substrate, and therefore the phase contrast of such areas will be darker than that of the PDES lamellae.

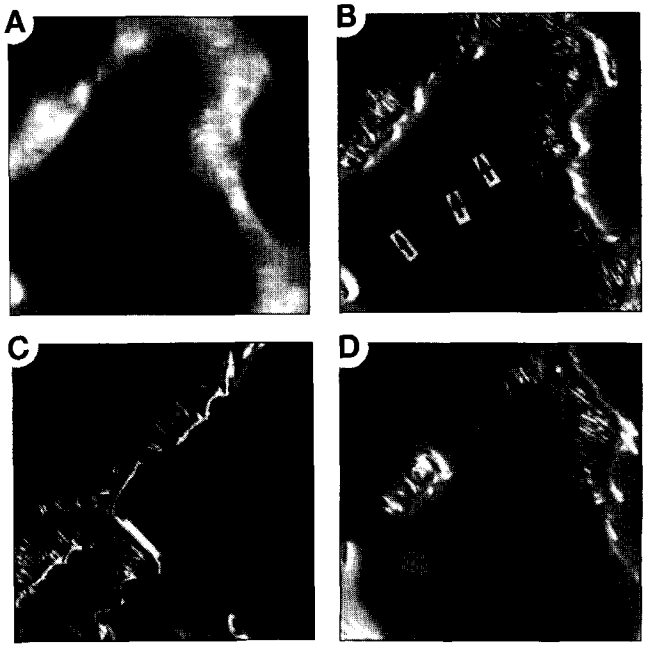


**Figure 6** (A)–(B) AFM height and phase images of a PDES sample at RT, (C) phase image of the same region as in (A)–(B) cooled to 263 K, (D) phase image of the same place as in (C) after warming to RT. The contrast covers height variations in the 0–500 nm range in (A), and phase variations in the 0–30 nm range in (B)–(D). Rubbing direction is from lower left to upper right. Arrows in (B) indicate thin polymer patches discussed in the text. In all images scan size is $14.5 \times 14.5\,\mu m^2$

These results allow us to interpret AFM images of PDES in terms of different stiffnesses of this polymer material in its amorphous and mesomorphic states. In a comprehensive image analysis it is also necessary to consider the possible effects of adhesion, which might also be different for amorphous and mesomorphic structures. However, the current understanding of the image contrast is sufficient for the study of the PDES structure.

*Structure of PDES in amorphous and mesomorphic states*

Several structural features of oriented PDES strands are seen in the images in *Figures 4A–D*. It is evident that a ratio of polymer parts in the amorphous and mesomorphic states depends on the size of the PDES patch. In the left part of the images in *Figures 4A–B* one sees PDES droplets, which are separately lying on the substrate and are preserved in the amorphous state. Lamellar structures common for PDES in the mesomorphic state dominate in the polymer strands in the right part of the image. A high magnification image recorded in the central part of the strand (*Figure 4C*) shows close packed nanostructures of 60–90 nm in width. Fine features of 20–30 nm in width are resolved on some of these nanostructures, and the number of such features is increased after cooling to 280 K (*Figure 4D*). It is reasonable to assign the fine features and the nanostructures, respectively, to lamellae standing edge-on and to their blocks. In these lamellae, polymer chains are oriented along the rubbing direction and parallel to the substrate plane. The nanostructures seen in small droplets in the left part of the images in *Figures 4A–B*, as well as the similar ones in *Figures 1A–C*, can be assigned to lamellae that lie flat and in which the PDES chains are oriented perpendicular to the rubbing direction and the substrate plane. The lamellae standing edge-on and the lamellae lying flat were identified earlier by optical and electron microscopy in isotropic PDES films[8a,9].

The morphological changes detected on cooling of PDES samples to 280 K reflect their complete conversion to the mesomorphic state. The phase image obtained at RT (*Figure 5A*) exhibits numerous lamellae which lie flat and which are embedded in the amorphous polymer. Only lamellar structures are seen in the PDES sample after cooling (*Figure 5B*). A similar trend is documented by the phase images in *Figure 6*, where the same part of a polymer sample was observed during a cooling–warming cycle. The height and phase images (*Figures 6A–B*) show that at RT this PDES sample is partially in the

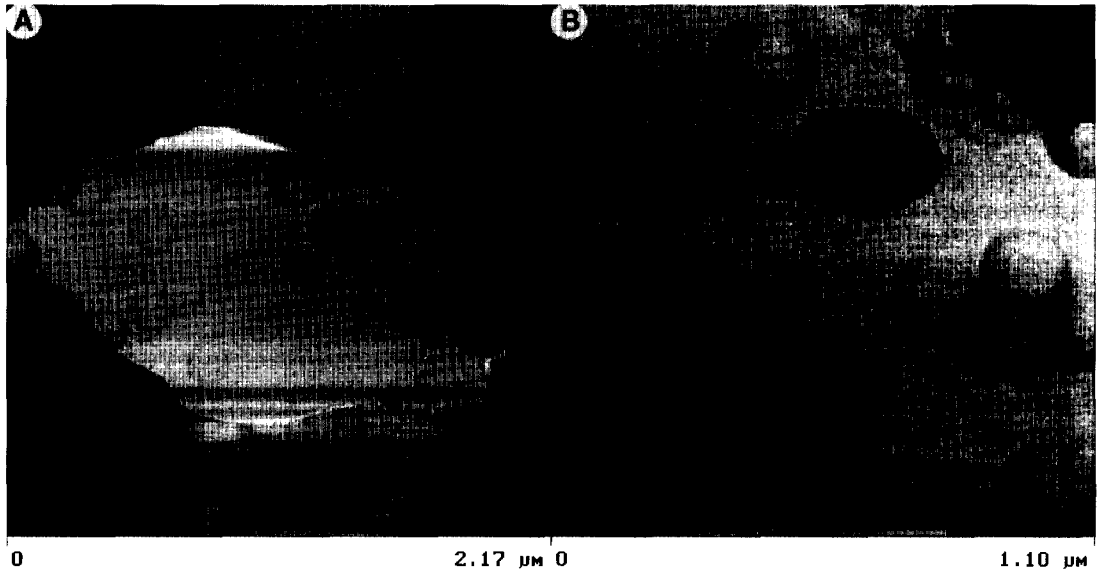


**Figure 7** (A)–(B) Phase images of one of the PDES patches indicated with arrows in *Figure 6*. The contrast covers phase variations in the 0–4° range in (A) and in the 0–2° range in (B)

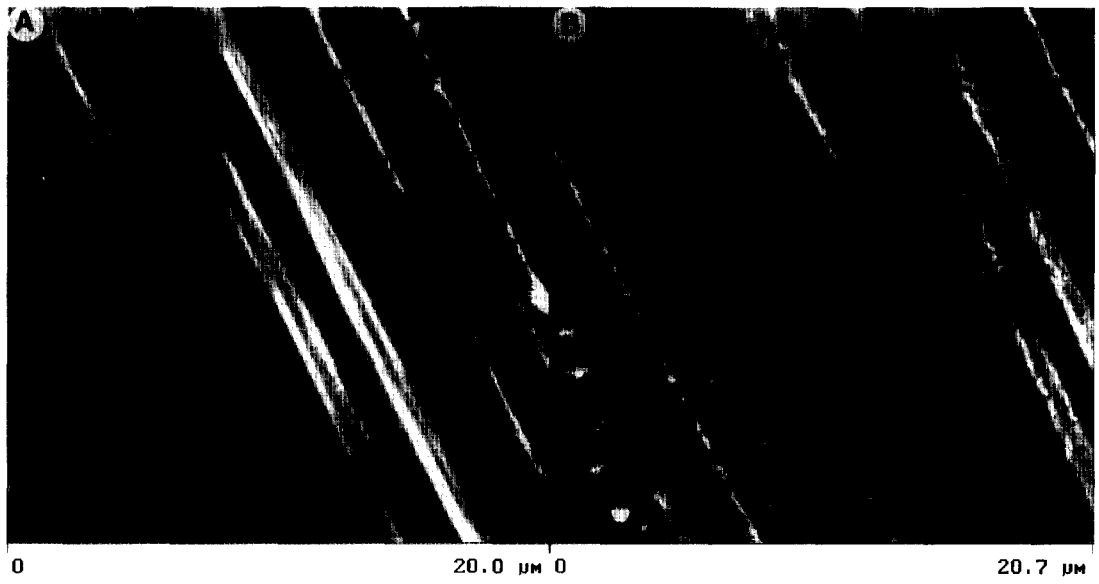


**Figure 8** (A)–(B) AFM height images of the same part of a PDES sample in the mesomorphic and crystalline states. The image in (A) was recorded at 283 K and the image in (B) at 268 K. The contrast covers height variations in the 0–200 nm range. Rubbing direction is from lower right to upper left

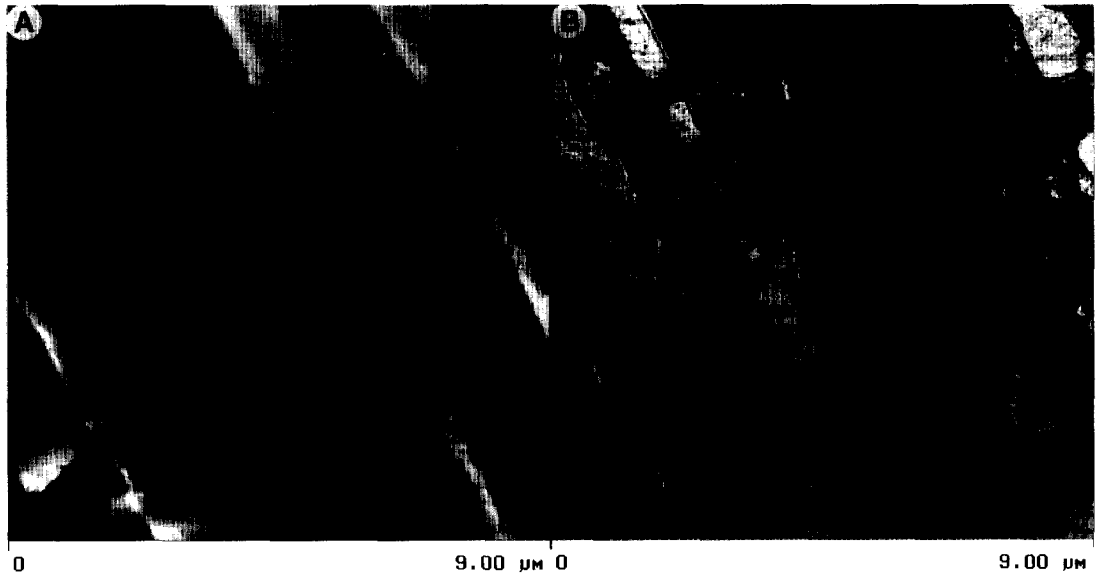


**Figure 9** (A)–(B) AFM height and phase image of PDES during crystallization at 268 K. The contrast covers height variations in the 0–150 nm range in (A) and phase variations in the 0–30° range in (B). Rubbing direction is from lower right to upper left

mesomorphic state and partially in the amorphous state. At low temperature lamellar structures dominate (*Figure 6C*), thus evidencing the conversion of the amorphous polymer to the mesomorphic state. On warming, a substantial part of the lamellar structures is melted, as seen from comparison of *Figures 6C* and *D*. It is worth noting that polymer in the patches (indicated with arrows) is still in the amorphous state at low temperature with the patches becoming broader. Due to the small height (*ca.* 5 nm) of the patches, they are barely distinguishable in the height image in *Figure 6A*. High magnification phase images in *Figures 7A–B* show that the patches are composed of fused discs 150–200 nm in diameter. This reveals the structural organization in the thin PDES patches, which is different from that in the mesomorphic phase.

*Solid–solid transition from mesomorphic to crystalline state*

By conducting AFM studies at low temperatures, we expected to monitor the transition from the mesomorphic to the crystalline state, which in bulk polymer occurs at temperatures around 273 K[7,8]. Morphological and nanostructure changes (which can be assigned to the similar transition in an oriented PDES layer on a Si substrate) have been observed in AFM images at temperatures close to 268 K. The morphology changes are seen in the height images in *Figures 8A–B*, which were obtained at different temperatures on the same part of the polymer layer. As we already know, the PDES layer in the mesomorphic state is characterized by strands oriented along the rubbing direction, and by the nanostructures oriented perpendicular to the rubbing

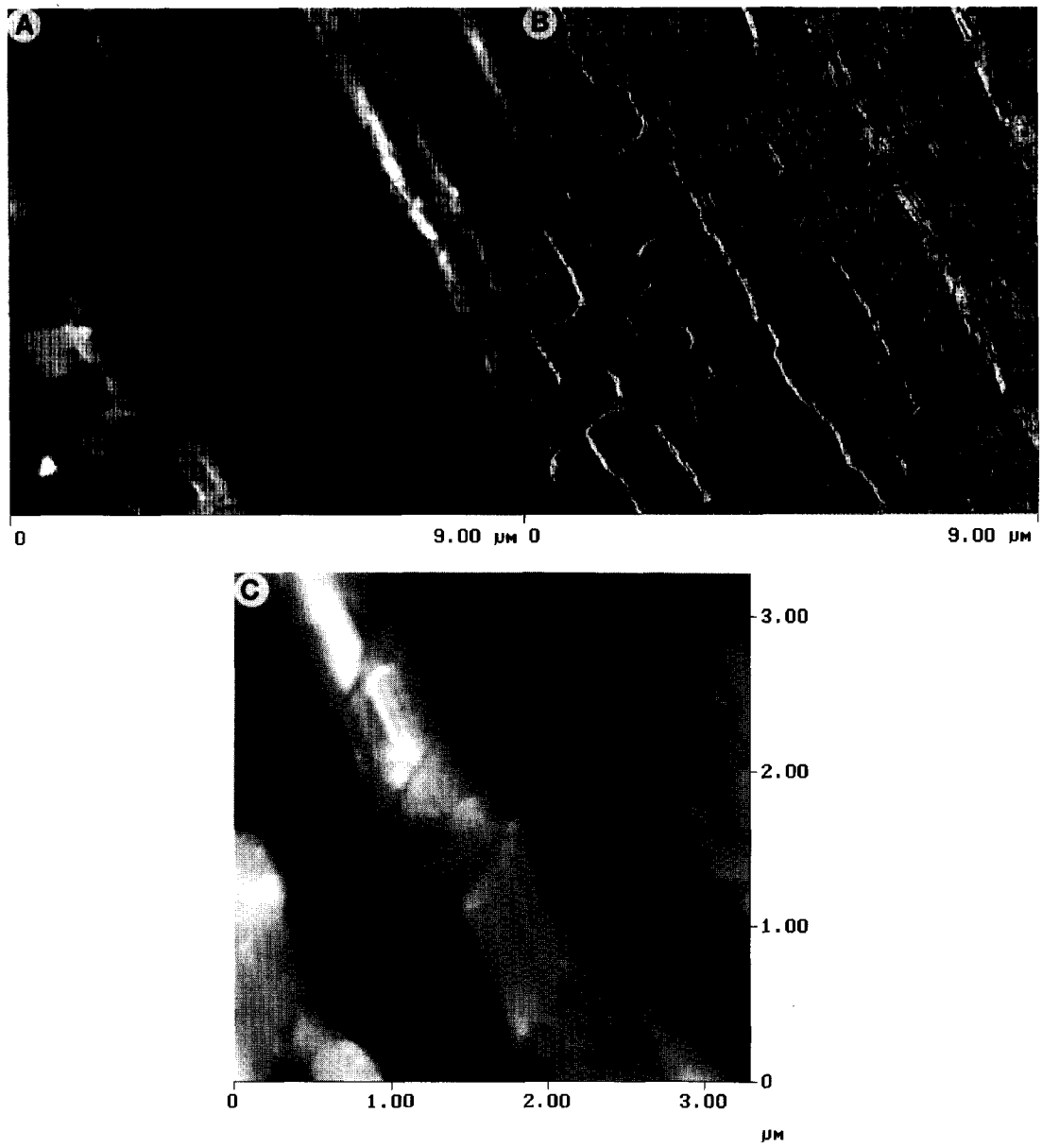


**Figure 10** (A)–(B) AFM height and phase images of crystalline PDES obtained at 268 K. (C) Zoomed part of the image in (A). The contrast covers height variations in the 0–170 nm range in (A) and in the 0–110 nm range in (C), and phase variations in the 0–10° range in (B). Rubbing direction is from lower right to upper left

direction (*Figure 8A*). After crystallization, the same sample region is composed of relatively flat ribbons, 300–1000 nm wide.

The crystallization process was slow enough to record the images showing a crystallization front (*Figures 9A–B*). In the right part of these images one sees lamellar structures of PDES in the mesomorphic state, whereas crystalline structures are distinguished in the left part. A sharp border separates the mesomorphic region from the crystalline region with nanostructures (*ca.* 50 nm in width) oriented along the rubbing direction. The images in *Figures 10A–B* show the same region after the crystallization was completed, with the phase image reveals only crystalline structures. Many ribbons seen in the height image (*Figure 10A*) have a shape with a sharp angle of *ca.* 60°, as seen from the zoomed part of this image, *Figure 10C*. This allows us to suggest a monoclinic crystalline structure in PDES crystals that is consistent with X-ray diffraction data obtained on stretched films of cross-linked polymer[9]. According to these data PDES crystallizes in a monoclinic modification with the following cell parameters: $a = 1.46$ nm, $b = 0.89$ nm, $c = 0.472$ nm, $\gamma = 29.66°$. Similar data were received for stretched films in the mesomorphic state but X-ray reflections are more diffuse than those for crystalline polymer. In the monoclinic structure PDES chains are extended along the *c*-direction, and there are two $(C_2H_5)SiO$-residues per identity period, which varies between 0.472–0.475 nm in the crystalline state to 0.488 nm in the mesomorphic state. Therefore, if we agree with the assignment of the flat ribbons observed in the AFM images to monoclinic polymer crystals, then PDES molecules in this sample are oriented perpendicular to the top surface. It is more difficult to explain the origin of the 50 nm wide crystalline nanostructures found in the phase images, which was also detected in the X-ray diffraction pattern of crystallized isotropic film[8b]. This substructure might be related to some density and stiffness variations in the crystalline sheets. We observed similar

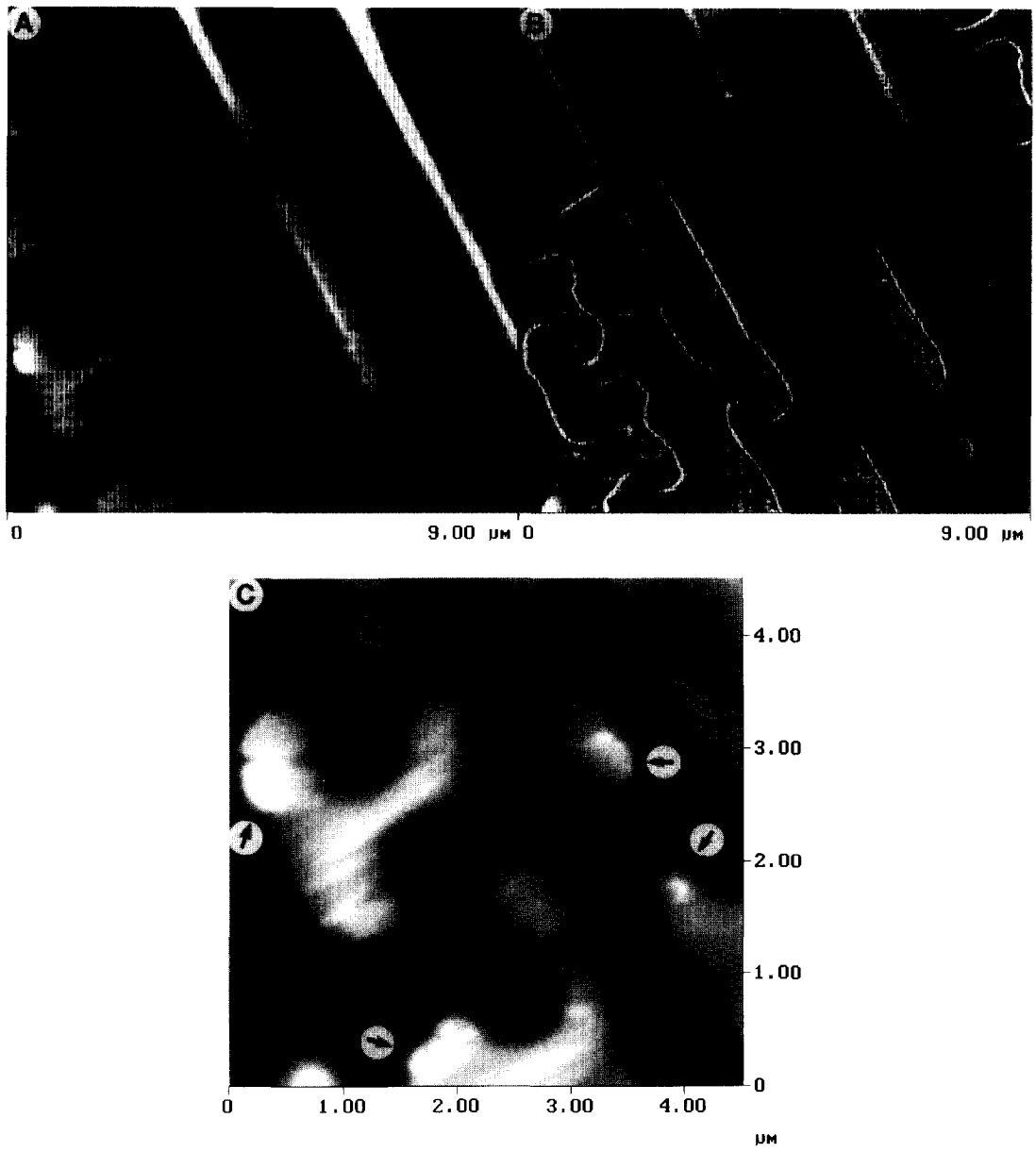


**Figure 11** (A)–(B) AFM height and phase images of crystalline PDES obtained at 273 K. (C) Zoomed part of the image in (A). The contrast covers height variations in the 0–185 nm range in (A) and in the 0–140 nm range in (C), and phase variations in the 0–10° range in (B). Rubbing direction is from lower right to upper left. The arrows indicate the PDES crystallites which appeared first

features in AFM images of single crystals of other polymers[12].

The present AFM results allow us to describe the crystallization process as the transformation of polymer lamellae found in the PDES mesomorphic state into lamellar crystals. This process proceeds relatively easily for the lamellae which are lying flat, but requires chain reorientation for the lamellae which are standing edge-on. Therefore, it can be expected that the crystallization is initiated on the surface, where space limitations are less severe than in the bulk. This expectation is confirmed by the images in *Figures 11A–C*, which were recorded when the sample was cooled to 273 K. Though these images show that most of the polymer is in the mesomorphic state, the crystalline structures appeared in several places. The flat triangular features (indicated with the arrows in *Figure 11C*), can be assigned to the PDES crystals and appeared first. The corresponding places in the phase image (*Figure 11B*) exhibit darker contrast than their surroundings which indicate greater stiffness of the crystalline regions.

## CONCLUSION

AFM images provide new information about the structure of PDES and its thermotropic structural transitions from the amorphous to the mesomorphic state and from the mesomorphic to the crystalline state. The phase images, whose contrast correlates to the stiffness of local surface regions, distinctly show lamellar aggregates in the mesomorphic state. At RT they are embedded in amorphous polymer. On cooling, they first convert into the mesomorphic state, and then crystallize. It has been found that the ratio of the amount of polymer in the amorphous and mesomorphic state, as well as the size of the nanostructures in the mesomorphic state, depends not only on temperature but also on the size of the polymer patch deposited on the substrate. There is

also evidence of nanoscale organization in thin amorphous patches separately lying on the Si substrate. Solid–solid crystallization of PDES from the mesomorphic state is accompanied by drastic changes of sample morphology and nanostructure. These changes suggest that molecular rearrangements accompany the crystallization of PDES.

To conclude, AFM applications to polymers are expanding from exploring surface morphology and nanostructure of relatively hard samples at RT to imaging of soft samples (like liquid crystalline materials), to examination of surface stiffness maps[4] and to imaging of thermotropic structural transitions. One can expect a broadened use of dynamic AFM techniques for studies of viscoelastic properties on the nanometre scale that will help to identify the structural units involved in the molecular relaxation processes inherent to polymers.

## ACKNOWLEDGEMENT

Monte Heaton (Digital Instruments) is acknowledged for his help in the preparation of this manuscript.

## REFERENCES

1 For a recent review, see: (a) Burnham, N. A. and Colton, R. in 'Scanning Tunneling Microscopy and Spectroscopy' (Ed. D. A. Bonnell), VCH, New York, 1993; (b) Magonov, S. N. and Whangbo, M.-H. 'Surface Analysis with STM and AFM', VCH Weinheim, 1996

2 (a) Leung, O. M. and Goh, M. C. *Science* 1992, **255**, 64; (b) Meyers, G. F., DeKoven, B. M. and Seitz, J. T. *Langmuir* 1992, **8**, 2330

3 (a) Wawkuschewski, A., Cantow, H.-J. and Magonov, S. N. *Adv. Mater.* 1994, **6**, 476; (b) Wawkuschewski, A., Crämer, K., Cantow, H.-J. and Magonov, S. N. *Ultramicroscopy* 1995, **58**, 185

4 Magonov, S. N. and Allen, M. Application Note, Digital Instruments, Inc.

5 Zhong, Q., Innis, D., Kjoller, K. and Elings, V. B. *Surf. Sci. Lett.* 1993, **290,** L688

6 (a) Maivald, P., Butt, H.-J., Gould, S. A. C., Prater, C. B., Drake, B., Gurley, J. A., Elings, V. B. and Hansma, P. K. *Nanotechnology* 1991, **2**, 103; (b) Radmacher, M., Tillman, R. W., Fritz, M. and Gaub, H. E. *Science* 1992, **257**, 1900

7 (a) Godovsky, Yu. K. and Papkov, V. S. *Adv. Polym. Sci.* 1989, **88**, 129; (b) Papkov, V. S. and Kvachev, Yu. P. *Progr. Coll. Polym. Sci.* 1989, **80**, 221

8 (a) Papkov, V. S., Svistunov, V. S., Godovsky, Yu. K. and Zhdanov, A. A. *J. Polym. Sci. Polym. Phys.* 1987, **25**, 1859; (b) Tsvankin, D. Ya., Papkov, V. S., Zhukov, V. P., Godovsky, Yu. K., Svistunov, V. S. and Zhdanov, A. A. *J. Polym. Sci. Polym. Chem.* 1985, **23**, 1043

9 Obolonkova, E. S. and Papkov, V. S. *High Mol. Compounds* 1990, **31**, 691

10 (a) Wunderlich, B. and Grebowisz, J. *Adv. Polym. Sci.* 1984, **60/61**; (b) Ungar, G. *Polymer* 1993, **34**, 2050; (c) Out, G. J., Siffrin, S., Frey, H., Oelfin, D., Kögler, G. and Möller, M. *Polym. Adv. Technol.* 1994, **5**, 796

11 Magonov, S. N., Kempf, S., Kimmig, M. and Cantow, H.-J. *Polym. Bull.* 1991, **26**, 715

12 Wawkuschewski, A., Crämer, K. and Magonov, S. N. Unpublished data